Off-line two-dimensional separation involving supercritical fluid chromatography for the characterization of the wastewater from algae hydrothermal liquefaction

Eloïse Teboul[1], Eliise Tammekivi[1], Magali Batteau[1], Christophe Geantet[2], Karine Faure[1,*]

[1] Université de Lyon, Institut des Sciences Analytiques, CNRS UMR 5280, 5 rue de la Doua, 69100 Villeurbanne, France

[2] Univ Lyon, Université Claude Bernard Lyon 1, CNRS, IRCELYON UMR 5256, F-69626 Villeurbanne, France , France

*corresponding author: Karine Faure; karine.faure@isa-lyon.fr

Keywords

Two-dimensional liquid chromatography;
supercritical fluid chromatography;
Off-line LC x SFC separation;
Microalgae;
Hydrothermal liquefaction

Abstract

An off-line multidimensional method involving liquid chromatography combined with supercritical fluid chromatography was developed for the characterization of the wastewater of hydrothermal liquefaction of microalgae *Chlorella sorokiniana.* The first dimension consisted of a phenyl hexyl column operated in reversed-phase mode, whereas the second dimension was performed on a diol stationary phase. Optimization of the kinetic parameters of the first and second dimensions were performed, taking into account the fraction collection system. The beneficial effect of working at high flow rate in both dimensions, as well as the need to work with short columns (50 mm) in the second dimension was evidenced. Injection volume was also optimized in both dimensions. The first dimension benefited from on-column focusing, while in the second dimension, untreated water-rich fractions could be injected without peak deformation. The performances of offline LCxSFC were compared to LC-HRMS, SFC-HRMS and LCxLC-HRMS for the analysis of the wastewater. Despite a long analysis time of 3.3h, the off-line separation coupled to high-resolution mass spectrometry exhibited a very large orthogonality with 75 % occupation rate of the separation space, reaching an effective peak capacity of 1050. While other evaluated techniques were faster, one-dimensional techniques failed to separate the numerous isomers while LCxLC exhibited lower orthogonality (45% occupation rate).

1. Introduction

Microalgae conversion is a promising technology for biofuel production. Among various thermochemical methods applied for converting algae biomass, hydrothermal liquefaction (HTL) is one possible conversion process that has the advantage of using wet raw material and moderate temperatures without the need for solvents. Therefore, it possesses a lower energy consumption than pyrolysis [1]. Among cultivated algae for biofuel production, *Chlorellacea* are very attractive species considering their resistance and fast-growing strains [2]. During the HTL process, the content of algae cells (lipids, proteins, and carbohydrates) is subjected to hydrolysis, deamination, and decarboxylation, leading to the production of compounds of interest for biofuel production. Furthermore, intermolecular reactions such as condensation and Maillard reaction lead to the formation of many polar compounds. The conversion results in two phases: a bio-oil that undergoes catalytic upgrading to produce paraffins, and an aqueous wastewater. This wastewater is rich in dissolved organic compounds, especially in N-containing molecules. It can be valorized further as a nutrient source for cultivating new algae [3-5], which reduces the economic footprint of algae conversion. However, the utilization of HTL wastewater has a dual effect on algae. It may slow down the algae growth but simultaneously increase the lipid content [6]. *Chlorella sorokiniana* showed the best adaptation to HTL wastewater as a growth medium [7]. The characterization of the HTL wastewater is of major importance to i) confirm the conversion pathways and optimize the HTL parameters, ii) select the algae strains and optimize their growth conditions, and iii) identify which compounds serve as nutrients and which compounds may have inhibitory effects on growth or the lipid yield.

The complex chemical composition of HTL wastewater has been demonstrated by detecting a large number of compounds with GC x GC-MS: cyclic nitrogen compounds such as pyrroles, indoles, pyrazines, and furans from amino acid condensation; phenols, ketones, and carboxylic acids from the decomposition of polysaccharides, piperazines and pyrrolidones from Maillard reaction between carbohydrates and basic amino acids [8-10]. While most of these molecules can be identified by using the NIST library, only 30 molecules have been quantified so far using GC-FID. Besides, the polarity of the organic acids or N-containing compounds and the aqueous nature of the wastewater may orientate the analyst towards liquid chromatography analysis. Thus, Lazzari et al. [11, 12] used LC x LC-HRMS to analyze the aqueous phase obtained from the pyrolysis of different biomasses, illustrating the power of two-dimensional separation for this purpose. However, the RPLC x RPLC setup showed some limitations in the orthogonality it could provide. Besides, to the best of our knowledge, the use of two-dimensional (2D) LC techniques has not yet been reported for the aqueous phase from HTL.

In this work, we evaluated the potential of using supercritical fluid chromatography (SFC) in combination with RPLC to analyze HTL wastewater from algae conversion. While RPLC in the first dimension is fully adapted to the separation of organic compounds dissolved in water, SFC on polar stationary phase shall provide an orthogonal separation mechanism, increasing the overall peak capacity compared to the RPLC x RPLC method.

The combination of LC and SFC has been scarcely implemented despite its high orthogonality, mainly because of the unavailability of commercial online instrumentation [13, 14]. Proof of concept online LCxSFC has been experienced in our group on the aqueous phase of pyrolytic oil [15] but it requires mobilizing simultaneously a LCxLC and a SFC instrument. On the other hand, off-line configuration can easily be implemented using two distinct instruments and providing a large set of information in just a few hours. The conditions used in both dimensions were optimized, using analysis time and effective

peak capacity as criteria. Careful considerations were brought on the subject of injecting LC fractions into the SFC so that there would be no need to modify the fractions between the two dimensions. The developed off-line LC x SFC-HRMS was then applied to the aqueous wastewater of the HTL conversion of *Chlorella sorokiniana.*

2. Material and methods

2.1 Chemicals and sample preparation

Acetonitrile (ACN) of HPLC grade was purchased from Honeywell Riedel-de-Haën (Seelze, Germany), formic acid (FA) and methanol (MeOH) (HPLC grade) were purchased from Merck (Darmstadt, Germany), and ethanol (EtOH) of HPLC grade was obtained from Fisher Scientific (Loughborough, UK). Water was obtained from an Elga water purification system (Veolia water STI, Le Plessis Robinson, France). Pressurized liquid CO_2 (99.995%) was obtained from Air Liquide (Pierre Bénite, France).

Chlorella sorokinania was grown under controlled conditions for 10 days and harvested by Dr. Delrue at CEA Cadarache (CTREG/DPACA, France). It was converted into bio-oil using the HTL process by Dr. Roubaud at CEA Grenoble (Biomass Technology Lab, LITEN, France). The aqueous phase was separated from the organic phase, then filtered through a Chromaphil Xtra PES 0.2 µm membrane filter, and stored at 5 °C.

2.2 Instruments

Agilent Infinity II 1260 LC system was equipped with a binary solvent delivery pump, an autosampler with a 900 µL loop, a column oven compatible with temperatures up to 90 °C, a diode array detector (DAD) with a 1 µL flow-cell, and a fraction collector with a capacity of 80 fractions. The maximum allowable flow rate was 4 mL/min and the maximum allowable pressure was 400 bar. Data acquisition was performed using Chemstation software (Agilent Technologies, Waldbronn, Germany). The extra-column variance and dwell volume were determined experimentally and found to be 36 μL^2 and 2.26 mL, respectively.

Agilent Infinity II 1260 SFC system was equipped with a binary solvent delivery pump, an Infinity II autosampler with a 100 µL loop, a column oven compatible with temperatures up to 85 °C, a DAD detector with a 2 µL flow-cell withstanding a pressure up to 400 bar, a back pressure regulator (BPR), and a make-up pump. The maximum allowable pressure was 400 bar. The dwell volume was measured in quasi-liquid conditions at 600 µL. Feed injection conditions were as follows: overfeed volume 4 µL, feed speed 1000 µL/min, and heptane as the feed solvent.

As the HRMS, an Agilent 6560 Ion-Mobility Quadrupole Time-of-Flight LC/MS equipped with a Jet Stream electrospray ionization (ESI) source (Agilent Technologies) was used.

Data acquisition was performed using Chemstation software (Agilent Technologies) and treated using MassHunter Qualitative 10.0. The 2D chromatograms were plotted using an in-house developed Matlab program from S. Heinisch and F. Rouvière.

2.3 Methods

The LC method was performed using a XSelect CSH Phenyl-Hexyl column (150 mm x 4.6 mm, 5 µm) on the Agilent Infinity II 1260 LC. The flow rate was 2.8 mL/min and the temperature was 30 °C. Final gradient conditions are displayed in Table 1. The injection volume was 500 µL. A set of 80 fractions were collected from the first dimension during the cycle time of 11.55 min, comprising gradient time, dwell time and dead time. Each fraction was collected every 0.14 min, providing a fraction volume of 392 µL, using the fraction collector on the Agilent Infinity II 1260 LC.

Four SFC columns purchased from Waters were screened: Torus 2-picolamine (2-PIC), 1-aminoanthracene (1-AA), diol (DIOL), and diethylamine (DEA) (all with dimensions of 100 mm x 3 mm, 1.7 µm), using a generic gradient elution (2% - 50% of methanol or ethanol as the co-solvent, normalized gradient slope of 5%). The temperature, the BPR, and the wavelengths were set respectively at 40 °C, 140 bar, 210 nm and 254 nm for all the experiments. The maximum flow rate allowed for all four columns was determined to be 1.1 mL/min when using 50 % co-solvent (generating around 400 bars). The final method was performed on a shorter DIOL column (50 mm x 3 mm, 1.7 µm) with a flow rate of 1.8 mL/min, as summarized in Table 1.

The 50-mm long SFC column was hyphenated to the MS using a "preBPR splitter with a sheath pump" configuration [16]. Briefly, the end of the SFC column was connected to a make-up pump delivering 2 mL/min of MeOH + 0.1% FA using a T-union. Then, the resulting flow was split using a second T-union. A low restriction tubing (170 µm, 90 cm) led most of the flow to the BPR, while a high restriction tubing (9 µm, 100 cm) decreased the flow rate entering the ESI source. The stainless steel tubing kit was provided by Agilent Technologies. In the final configuration, an additional pump was connected via a third T-union, delivering MeOH + 0.1 % FA to the MS at 200 µL/min.

The ESI source settings were the following: drying gas temperature, 300 °C; drying gas flow rate, 11 L/min; nebulizer pressure, 40 psi; sheath gas temperature, 350 °C; sheath gas flow rate, 11 L/min; fragmentor voltage 185 V; capillary voltage, 3500 V. Mass spectra data were collected in full scan mode with a mass range of 100-1700 *m/z* (with 18920 FWHM resolution at *m/z* = 322) and an acquisition rate of 10 spectra/s. No collision energy was employed during the MS data collection. The accurate mass of the precursor ion was recorded with a mass tolerance of ± 2 ppm.

3. Results and discussion

The off-line configuration allowed the use of commercially available instruments and decoupled both separation times and mobile phase flow rates between the two dimensions. This means that the stationary and mobile phases of each dimension could be screened individually and that the geometry of the columns can also be very different. Hence, the first dimension should be set on a column with a large volume, facilitating the work of fraction collection systems while limiting the impact of the external variances of the instrument on the chromatographic performances. The second dimension geometry has to be much smaller so that the flow would be adjusted for the hyphenation with MS while the overall separation time is kept reasonable.

3.1 Development of the first dimension (^{1}D) separation method

Based on a previous study [15], the phenyl hexyl stationary phase was selected according to its theoretical orthogonality with SFC stationary phases investigated here [17]. A scouting analysis of the sample was performed at 1% gradient steepness over the range 1%- 80% ACN, on a 150 mm x 4.6 mm column to facilitate fraction collection. It was revealed that the detected compounds eluted in a range of 1% to 30% ACN, indicating that the molecules present in the aqueous phase of HTL exhibit medium to high polarity. The ^{1}D operating conditions were optimized so that the overall peak capacity of the 2D separation was maximized. According to the linear solvent strength theory [18], the theoretical peak capacity in the first dimension n_{th} can be estimated by

$$n_{th} = 1 + \frac{\sqrt{N}}{4}\frac{1}{2.3\ sS+1}\ln\left(\frac{2.3\ sS+1}{2.3\ sS}e^{2.3\ S\Delta C} - \frac{1}{2.3\ sS}\right) \qquad (1)$$

Where *N* is the column efficiency, *S* the slope of the retention model, *ΔC* the elution composition range, and *s* the ^{1}D gradient steepness.

However, the first dimension undergoes sampling after the elution, which has deleterious effects on the resolution of peaks. It is generally conceived that a peak should be sampled 3 to 5 times. But in most online LC x LC separations, this recommendation is usually not followed. Indeed, in online configuration the sampling time equals the second dimension duty cycle. Reducing the sampling period would induce a reduction in the second dimension gradient time that limits the peak capacity of the second dimension. In off-line configuration, there is no such constraint on sampling time as the two dimensions are decoupled in time and the number of fractions is only limited by the instrumental constraints. Using Monte Carlo simulation of Gaussian peaks, Davis et al. evaluated the impact of undersampling on the peak capacity obtained after collection (n_s) as Equation 2 [19]

$$n_s = \frac{n_{th}}{\sqrt{1+0.21\left(\frac{t_s}{\sigma_t}\right)^2}} \qquad (2)$$

With $\sigma_t$the average peak standard deviation in time units and t_s the sampling time, corresponding to the time required to collect a fraction in a vial.

When approximating that the peaks are homogeneously distributed along the gradient time t_g, the theoretical peak capacity n_{th} can be expressed as:

$$n_{th} = \frac{t_g}{4\sigma_t} \qquad (3)$$

In a comprehensive mode, the collection has to be performed along the whole separation space, here during t_g. The number of fractions n_f required in a comprehensive mode is therefore:

$$n_f = \frac{t_g}{t_s} \quad (4)$$

Combining equations (2), (3), and (4), the effective peak capacity after sampling in off-line configuration can be expressed as a function of the theoretical peak capacity and the number of fractions (5)

$$n_s = \frac{n_{th}}{\sqrt{1+3.36\left(\frac{n_{th}}{n_f}\right)^2}} \qquad (5)$$

By plotting the percentage of the remaining peak capacity $\frac{n_s}{n_{th}}$ vs. the ratio of the number of fractions over the theoretical peak capacity $\frac{n_f}{n_{th}}$ (Figure 1a), it can be observed that a goal of 80% remaining peak capacity requires that the number of fractions exceeds the theoretical peak capacity by a factor 2.5. This objective is far from being reached, as off-line LC x SFC publications often report collection of only 40-50 fractions [20, 21], a number that is surprisingly low since fraction collection systems offer between 80 and 120 vials, depending on the manufacturer. The undersampling effect is often not taken into account for determining the effective peak capacity of the off-line 2D approach while it is systematically done in the optimization of online LC x LC [22, 23].

The theoretical peak capacity on a typical HPLC column geometry of 4.6 x 150 mm; 5 µm particle size, can be estimated using equation 1 (Figure 1b). It relates both to the square root of efficiency and to the gradient steepness, and so depends on flow rate and gradient time. Increasing the flow rate from 0.7 mL/min (optimal flow rate) to 2.8 mL/min (maximal flow rate) on the LC column led to an expected loss of observed efficiency, from 10400 plates to 6600 plates, while for the same gradient time, increasing the flow rate decreased the gradient steepness. Theoretical peak capacity for the two flow rates was plotted as a function of gradient time (Figure 1b) and showed that using the 4.6 mm x 150 mm; 5 µm column geometry, it was more beneficial to work at large flow rate. Theoretical peak capacity was estimated between 50 and 140 for a gradient time between 3 min and 60 min (Figure 1b). Keeping 80% effective peak capacity (Equation 5) would require between 125 and 700 fractions, that would not only being difficult to handle technically, but also would result in an unreasonable ^{2}D analysis time. Figure 1b reports the effective peak capacity obtained after sampling when using a collection system with 80 fractions. The method development in online LC x LC tends to suggest that the ^{1}D gradient time should be quite long, usually 30 to 60 min, so that the peak broadening in the first dimension would allow a longer sampling time corresponding to the ^{2}D cycle time. On the contrary, in off-line mode, the maximal peak capacity obtained after sampling is reached for short gradient times (Figure 1b). In the present work, using a collection system of 80 fractions, a 10 min gradient performed at maximal flow rate was sufficient to reach the maximal peak capacity of 41 (Figure 1b). Using another collection system allowing 100 fractions would increase the peak capacity after undersampling to a value of 50. With these selected gradient time and flow rate, the gradient range was adjusted to 1%-40% ACN, so that according to the new normalized gradient slope, all the compounds eluted during the gradient. The composition at elution of the last peak was evaluated to be 33 % ACN in these conditions.

Thanks to the aqueous nature of the algal HTL waste and the use of an RPLC method in the first dimension, on-column focusing allowed large injection volumes, thus increasing sensitivity without compromising the chromatographic performances. Injection compression factor is related to the ratio between two solute retention factors: k_s, obtained with the injection solvent, here 100 % water, and ke, obtained with the mobile phase at elution. [24]. With a sample in 100% water and a gradient starting at 1 % ACN, the compression factor is expected to be over 1 and increasing with the solute retention. Three distinct peaks distributed in the first half of the chromatogram were monitored using UV detection at 254 nm (Figure 2a). The peaks eluting before Peak 1 were not sufficiently resolved to measure their peak width. The peak capacity calculated for these three peaks when injecting increasing volumes was compared to the peak capacity obtained when injecting 100 µL, corresponding to 5.8% of the column volume (Figure 2b). Peak broadening when injecting over 200 µL resulted in a peak capacity decrease as expected. While Peak 1 (9% ACN at elution) and Peak 3 (17% ACN at elution)

followed the same variation, with a loss of only 20% in peak capacity, Peak 2 (16% ACN at elution) exhibited a much larger loss. An injection volume of 500 µL (30% of the column dead volume) was selected, hence keeping more than 70% of the peak capacity for compounds eluting with over 9% ACN. The broadening of compounds with a composition at elution lower than 9% ACN could not be monitored using the ^{1}D LC-UV system because of co-elution, but the 2D chromatograms developed thereafter showed their peak width remained similar to more retained compounds.

The variability of the first dimension separation was assessed in the final conditions, stated in Table 1, by monitoring the peak width and retention time of 10 peaks spread over the gradient. A sequence of 5 injections was performed on three different days. The intra-day standard deviation of retention time was below 0.01 min for all 10 peaks. The inter-day standard deviation of retention time was below 0.05 min for all peaks, reaching only 0.01 min for 80% of the compounds.

The average peak width at 4σ was measured at a value of 0.11 min ± 0.02 min, so the experimental peak capacity before fraction collection was estimated using equation 3 and the experimental peak width, at a value of 67. Using an 80-vials fraction collector, the ^{1}D effective peak capacity corrected by the undersampling (Equation 5) was 37, quite close to the value of 41 calculated with theoretical performances (Figure 1b). The difference may be explained by the instrumental variance generated by the collector that was not taken into account in the theoretical calculation.

3.2 Development of the ^{2}D SFC method

The initial screening was performed on four 100 mm long columns with various stationary phases, namely 2-PIC, 1-AA, DIOL and DEA, using methanol or ethanol as co-solvent B, a generic gradient (2-50% B), and a normalized slope of 5% (Figure S1). The sample was initially diluted in 85:15 water/ACN (v/v) to simulate the composition of a fraction collected after the first dimension. The columns based on 1-aminoanthracene and diethylamine were found to be too retentive, leading to uneluted compounds that were removed from the column after flushing it with 100% organic solvent. We suppose that the non-eluting compounds are acidic, as an excessive retention on amino-based stationary phases has already been reported for this class of compounds [25]. The chromatographic profile obtained using 2-PIC and DIOL columns were similar, with a slightly higher retention on DIOL column. Using a lower gradient steepness of 1% and an initial composition of 2 % organic solvent, the separation space offered by the DIOL column was investigated for various co-solvent compositions (Figure S2). Compounds were detected in the range of 2% - 29% using MeOH as the co-solvent and 2% - 37% using EtOH as the co-solvent (Figure S2a). The effect of additives in the EtOH co-solvent such as 0.1% formic acid or 2% water was found to have minor impact on the quality of the separation (Figure S2b). Therefore, ethanol was selected as the co-solvent.

The performances of the off-line 2D separation were simulated for various sets of LC and SFC conditions. The LC flow rate was 2.8 mL/min. The ^{1}D gradient time was allowed to vary between 3 min and 60 min. The calculations were performed for 60, 80 or 100 fractions. The ^{2}D column length was either 50 mm or 100 mm. The ^{2}D flow-rate was fixed at the maximal allowable column pressure drop (i.e. 400 bars) when reaching the maximal co-solvent content, corresponding to 1.8 mL/min on a 50 mm long column and 1.1 mL/min on a 100 mm long column. The ^{2}D gradient time was allowed to vary between 1 min and 10 min. Other conditions were as reported in Table 1.

The theoretical peak capacity of the 2D off-line separation $n_{2D,theo}$ and the overall analysis time t_{2D} were the selected criteria.

The theoretical peak capacity $n_{2D,theo}$ is the result of the product of the theoretical peak capacities from each dimension, corrected by the undersampling after the ^{1}D collection (Equation 6). In a first approach, the injection effects and the instrumental variances were not included in the calculation.

$$n_{2D,theo} = n_s * n_{SFC} \quad (6)$$

The theoretical peak capacity of the LC separation, after fraction collection n_s, was calculated using equation 5. The theoretical peak capacity of the SFC separation n_{SFC} is difficult to model as the density increase that undergoes the mobile phase during the gradient may impact the efficiency. For example, working at a flow rate of 1.8 mL/min on a 50 mm column, the column efficiency was measured at 7400 plates for 2% EtOH as co-solvent and at 4700 plates when the mobile phase contained 50% EtOH. For a first estimation, Equation 1 was used for calculation, with an average efficiency. Better approximation should require a deeper investigation on the modeling of kinetic performances of SFC in gradient mode.

The duration of the offline 2D analysis t_{2D} is the result from the ^{1}D gradient time and the sum of the ^{2}D cycle times for analyzing the LC fractions in a comprehensive mode (Equation 7).

$$t_{2D} = \left({}^1t_{dwell} + {}^1t_0 + {}^1t_g \right) + n_f \times \left({}^2t_{inj} + {}^2t_{dwell} + {}^2t_0 + {}^2t_g \right) \quad (7)$$

With ${}^it_{dwell}$, ${}^it_0$ and ${}^it_g$ the dwell time, the dead time and the gradient time of dimension *i*, respectively. The injection duration in second dimension ${}^2t_{inj}$ is a fixed value depending only on the SFC injection design. The Agilent SFC instrument incorporates a feed injector, aimed at pressurizing the sample before introduction along the mobile phase flow [26]. The duration of the injection process ${}^2t_{inj}$ using this instrument was estimated to be 0.56 min (average of 10 measurements).

The calculated performances of the offline LCxSFC separation are represented in Figure 3. As could be expected, an increase in theoretical peak capacity may be achieved at the expense of longer analysis time, whether increasing the first or the second dimension gradient time. However, the ^{1}D gradient time had a limited impact on the performances with an optimum at 10 min whatever the set of conditions, as observed previously, whereas the ^{2}D gradient time (colors in Figure 3) had a major impact on both peak capacity and analysis time. For example for 80 fractions, the optimized theoretical peak capacity was 3359 for 159 min (^{2}tg 1 min), 3866 for 234 min (^{2}tg 2 min) and 4994 for 479 min (^{2}tg 5 min). Secondly, the number of fractions collected had a major impact on both performances criteria. Finally, it appeared that the shortest column, i.e. 50 mm (circle symbols in Figure 3) provided better results than the longest one for short ^{2}tg. This may due to the beneficial impact of shallow gradients despite a loss in column efficiency. Nonetheless, the two trends where very similar for ^{2}tg equal 10 min. Using a longer SFC column should be advantageous when peak capacity higher than 5000 are required, but at an expense of analysis time over 16 hours.

In the light of the above, the LC gradient time was set to 10 min and the number of fractions to the maximum allowed by the available instrument. The second dimension was performed on a 50 mm long column at a maximal flow rate of 1.8 mL/min. For an analysis time of 200 min, the gradient time of the second dimension was set at 1.34 min (equation 7) considering an injection time of 0.56 min, a step to return to initial composition in 0.12 min (corresponding to one column dead time) and a hold time at initial composition for 0.33 min (corresponding to the instrument dwell time). In these conditions, the theoretical peak capacity was estimated at 3587.

The SFC instrument was then coupled with HRMS using a commercial pre-BPR splitter with a make-up pump interface that has been proven optimal for the ESI source [27]. Methanol + 0.1% FA was added as the make-up solvent to further improve the MS signal. The solvent flow rate entering the MS source can be calculated using the equations described by Guillarme et al. [16], adapted in our work to the viscous binary mixture of ethanol and methanol. Simulations were performed for the initial mobile phase composition (2% EtOH in CO_2) and for the final mobile phase composition (50% EtOH). When the make-up flow was below 600 µL/min, the flow was directed entirely to the MS and the BPR system experienced an issue with maintaining stable pressure. Increasing the make-up flow resulted in an increase in the split ratio. At initial composition, the flow of solvent entering the MS slightly increased with the make-up flow while the flow of CO_2 drastically decreased (Figure S1). Using a make-up flow of 2000 µL/min resulted in an initial flow of solvent entering the MS at 760 µL/min. The overall flow, including SFC eluent and make-up flow was splitted by 2.7, from 3800 µL/min to 1419 µL/min into the MS. Unfortunately, the MS signal was not repeatable at the beginning of the gradient in these conditions, despite using a caloratherm at 60 °C to avoid freezing the tubing. Using an additional pump delivering 200 µL/min as proposed by Crepier [28] prevented solute precipitation by reducing the CO_2 content to 40%. At the final gradient composition, the viscosity of the eluent was much higher, leading to a more important split of flow, estimated at a value of 4.6 (Figure S3). The flow of CO_2 entering the MS tubing was low, calculated at 196 µL/min and no freezing or precipitation was noted. With a final 2000 µL/min make-up flow and a 200 µL/min additional flow, the amount of organic solvent entering the MS source remains almost constant through the gradient (960 µL/min at initial gradient conditions and 850 µL/min at final gradient conditions). Meanwhile, the composition of the organic solvent entering the source evolved with the chromatographic gradient, with a ratio 4:96 EtOH/MeOH (v/v) at initial composition and 53:47 EtOH/MeOH (v/v) at final conditions, which had no major influence on the MS response.

The peaks were spread over the whole range of co-solvent (Figure S4) with very different profiles according to detection modes. The molecules responding in positive ESI-MS mode eluted between 0.6 min and 2 min, whereas peaks detected in ESI-MS negative mode eluted mostly between 0.4 min to 1.2 min, and peaks eluting between 0.2 min and 0.4 min were only detected in UV. This observation clearly illustrated the diversity of molecules and the need for three detection modes.

Because isolated peaks could not be distinguished using this short SFC separation, the maximal volume that could be injected into the SFC had to be determined using extracted ion chromatograms (EIC). The fractions collected from the first dimension were in a composition ranging from 99% to 60% water. As the sample was not soluble in aprotic solvents, it was decided to inject the fractions without any treatment. With the objective of increasing the sensitivity, increasing volumes of sample diluted in water/ACN with either 80% or 50% water were injected in the ^{2}D conditions. Two peaks were monitored, one eluting in the early part of the gradient, at 8% co-solvent (*m/z* 184) and the other one eluting at 18% co-solvent (*m/z* 151), after the water peak, which eluted at 15% co-solvent (1.01 min). The retention time of the early eluting peak increased linearly with the injected water volume (Figures 4a and 4b). Nonetheless, the peak width was not affected by the content of water and the peak capacity was found to be higher when the diluent contained more water (Figure 4e). This phenomenon resulted from the higher retention of water molecules than of early eluting compounds on the polar stationary phase of SFC [29]. As expected, the compounds eluting after water molecules were much

more affected by the content of water in the diluent. The content of 80% water in the diluent (corresponding to the fractions eluting at the beginning of the ^{1}D gradient) did not produce any retention shift of the highly retained compound. However, the increase in volume had a detrimental effect on peak width, with peaks broadening when 10 µL were injected and peaks splitting when 20 µL were injected (Figure 4c). With a lower water content in the diluent (50%, corresponding to the composition at the end of the ^{1}D gradient), peaks were broadening in a more typical way, without any splitting (Figure 4d). Therefore, to maintain 70% of the peak capacity in SFC, whatever the variation of diluent of the fractions eluting from the ^{1}D gradient, it was decided to limit the injection volume in the second dimension to 10 µL. Because the peak widths had to be measured on EIC, the experimental peak capacity took into account the dispersion generated by the electrospray source. Under these injection conditions, the average peak width at 4σ was measured 5 times for the peak eluting before water, i.e., before 1.0 min at a value of 0.039 min and for 5 peaks eluting after water at a value of 0.050 min. Hence, the experimental peak capacity reached between dead time and 1.0 min was estimated at 22, while the experimental peak capacity in the second part of the SFC chromatogram was estimated at 16.

3.3 LC x SFC-HRMS analysis of the HTL wastewater

Applying the final conditions (Table 1), the wastewater from the HTL of *Chlorella sorokiniana* was analysed by off-line LC x SFC-HRMS. The total time could be divided into a 10 min ^{1}D separation and 80 times 2.35 min (^{2}D cycle time), yielding an overall analysis time of 3.3 h. The 80 resulting chromatograms were compiled in an in-house developed Matlab program to plot a 2D chromatogram (Figure 5). The final chromatographic profiles that were obtained in the range 100-1700 *m/z* in negative ionization mode (Figure 5a) and positive ionization mode (Figure 5b) were quite dissimilar, suggesting the interest in keeping both ionization modes. This was expected given the wide diversity of molecular structures present in algae wastewater, with N-containing compounds and O-containing compounds having very different ionization responses in the ESI source.

The peak broadening due to injection effects during transfer was confirmed by monitoring the peak width (expressed here as FWHM) of 4 isolated peaks detected in negative mode, noted 1 to 4 in Figure 5a. Peaks eluting in the left part of the contour plot, i.e., with ^{2}D retention time below 1.2 min (Peaks 1 and 2), exhibited low peak width whatever their position in ^{1}D, measured at 0.022 min and 0.023 min for peak 1 and peak 2, respectively. Peaks eluting in the first part of the ^{1}D LC ($^{1}t_R$ below 5 min, i.e., fraction 30) and with $^{2}t_R$ over 1.2 min (bottom-right in Figure 5) were very broad due to the transfer of diluent with high water content. For instance, peak 3 exhibited a width of 0.036 min. Finally, the molecules retained in both LC and SFC (top-right in Figure 5) were well resolved, with peak 4 displaying a width of 0.024 min. Overall, it can be concluded that when fractions contained high amounts of water, only one-quarter of the elution space (bottom-right in Figure 5) exhibited broader peaks, for which the impact on peak capacity was limited to around 30% of loss compared to the other peaks.

The resulting 2D plots show that the developed LC x SFC method has large orthogonality, with the peaks spread over the entire separation space. The high orthogonality is caused by highly different retention mechanisms, as LC retention is based on dispersive and π-π interactions while SFC retention is based on dipole-dipole interaction. In negative mode, a downward diagonal was observed (Figure

5a), implying that the retention mechanisms are of opposing forces on the compounds responding in this ionization mode. However, the molecules responding in positive ionization mode (Figure 5b) were distributed evenly over the separation space. The orthogonality performances were calculated using the asterisk method [30], taking into account all detection modes. The results in Table 2 show that each dimension was well used, with peak spread over 90%. As already observed in Figure 5, there was no direct correlation between the two dimensions, as demonstrated by the absence of clustering along the upward diagonal. On the other hand, a certain degree of clustering could be detected along the downward diagonal, but its extent seemed quite low, with a 75% peak spread around this vector. According to the asterisk method, the overall occupation rate γ was 75%, while a convex hull method [31], much simpler to implement, slightly overestimated this value to be 78%.

The predicted effective peak capacity was estimated (equation 8) as the theoretical peak capacity corrected by *i)* the external variances due to the injection effects in LC, β_{LC}, and in SFC, β_{SFC}, both values being set at 70%, and *ii)* the overall occupation rate γ. The predictive effective peak capacity was calculated at 1318.

$$n_{2D,pred.} = n_{2D,theo} * \beta_{LC} * \beta_{SFC} * \gamma \quad (8)$$

Taking into account experimental peak widths in both dimension, undersampling with 80 fractions, and orthogonality, the experimental effective peak capacity of this method was estimated at around 1050 for an overall analysis time of 200 min (3.3 h). The discrepancy between prediction and experimental value may come from the effect of external variances and the bias from LSS hypothesis on SFC separation.

This experimental value was compared to one-dimensional techniques, either LC-HRMS or SFC-HRMS or to the two-dimensional online LCxLC-HRMS, all in optimized conditions. Both one-dimensional separations were carried out on 100 mm long column at a 1% gradient steepness to maximize peak capacity while limiting dilution. The best LC separation was achieved in 15 min (Figure S5a) and provided 122 in peak capacity whereas the best SFC separation was achieved in 30 min (Figure S5b) and provided 250 as experimental effective peak capacity. Online LCxLC was considered in two different configurations. The first one consisted in the use of fluorophenyl stationary phase in the first dimension while the second configuration used phenylhexyl in the first dimension. Both configurations used ACN and formic acid as ^{1}D mobile phase. The ^{2}D column was a Cortecs C18 with MeOH and ammonium acetate as 2D mobile phase. While these configurations were selected to maximize orthogonality, there was still a large correlation of the retention behaviour in both dimensions (Figure S6) as expected from RPLC x RPLC combinations. Peaks responding in ESI + occupied at best 45% of the available separation space (calculated on phenylhexyl x C18 combination), very similar to the occupation rate found by Lazzari et al. [11] for the analysis of aqueous phases using other LCxLC combination. Nonetheless, the effective peak capacity generated by LCxLC reached 1190 in 30 min, but required a specific instrumentation.

The developed LC x SFC-HRMS technique could be used for a non-target analysis to compare the wastewater composition resulting from different HTL processes or from different algae strains. However, this kind of study would require a large number of replicates to get statistically representative results due to the versatility of plant demography, in which case a faster online strategy could be preferred. On the other hand, a two-dimensional separation hyphenated to high-resolution mass spectrometry is of interest for target analysis by reducing matrix effects and improving separation

of isomers. An off-line configuration offers a quick access, without dedicated instrumentation, to a highly discriminative analysis. Once the position of the target is elucidated using a comprehensive analysis, the separation can be restricted to elution zones of interest, and fraction analysis can be completed *a posteriori* if necessary. The interest of the LC x SFC method over a one-dimensional method can be illustrated through the monitoring of molecules whose content in the wastewater used for algae cultivation is suspected to have an impact on either the algae's growth or lipid yield. For example, Figure 6 shows the extracted chromatograms of ion *m/z* 247.1447. This ion corresponds to the molecular ion of 3-benzyl-6-isopropyl-2,5-piperazinedione. Piperazinediones are generated from the recombination of amino acids present in the algae during the hydrothermal liquefaction. They represent a beneficial source of nitrogen for algae cultivation on wastewater. However, after reaching the optimal growth, a prolonged N-starvation induces the production of starch and lipids for energy storage in the cells. If the N-starvation is prolonged, then lipids accumulate while the starch content decreases [32]. Consequently, the intake of piperazinediones should be strongly controlled during N-starvation. The one-dimensional LC-HRMS analysis exhibited a cluster and two distinct peaks with a signal-to-noise ratio above 10 (Figure 6a), while the SFC-HRMS analysis retrieved two main peaks in a much noisier baseline (Figure 6b), that would not allow any quantitative analysis. The two-dimensional LCxLC analysis (Figure 6c) exhibited 9 spots with a signal-to-noise ratio over 10, demonstrating two-dimensional separation reduced matrix effects that strongly inhibited MS signal when only one separation dimension was used. Nonetheless, a cluster was still present (around 10 min in the first dimension) with a diagonalization suggesting that despite a larger peak capacity, the peaks with the same m/z ratio were not fully resolved. The 2D LCxSFC chromatogram with its higher orthogonality compared to LCxLC (Figure 6d) exhibited 14 spots with a signal-to-noise ratio over 10 at this specific m/z ratio, offering a better characterization of these potential isomers or compounds with similar fragments.

Conclusion

In this study, an off-line 2D RPLC x SFC-HRMS method was developed and proved to be a powerful tool for the characterization of HTL wastewater of algae.

The wastewater was directly introduced into the first RPLC dimension without any sample treatment. Injection volume was maximized up to 30% of the column dead volume. Repeatability and intermediate precision of the ^{1}D separation were assessed. The theoretical estimation of fraction collection highlighted the importance of the number of fractions while underlining the limitation in peak capacity performances of an off-line approach. The ^{2}D SFC separation was optimized in terms of stationary phase, mobile phase, and hyphenation to HRMS. The comprehensive LC x SFC-HRMS analysis of HTL wastewater from *Chlorella sorokiniana* illustrated the large orthogonality of the 2D method, with a large occupation of the separation space. Using 80 fractions, the overall peak capacity reached 1000.

The developed off-line LC x SFC-HRMS method could be used for non-target analysis but also to facilitate target analysis thanks to the ability to decrease matrix effects and separate the numerous isomers present in HTL wastewater.

Acknowledgments

This work was funded by the French national agency for research (RafBioAlg ANR-18-CE43-0009). The authors thank Adriana Ramirez and Dr. Florien Delrue from CEA Cadarache (CTREG/DPACA) for the cultivation of *Chlorella sorokiniana* algae and for interesting discussions about their growth behavior in HTL wastewater. The authors also thank Dr. Anne Roubaud and Lucie Matricon from CEA Grenoble (Biomass Technology Lab, LITEN) for providing wastewater from HTL-processed algae.

References

1. D. López Barreiro, W. Prins, F. Ronsse, and W. Brilman, Hydrothermal liquefaction (HTL) of microalgae for biofuel production: State of the art review and future prospects. Biomass and Bioenergy, 2013. 53: 113-127.DOI: https://doi.org/10.1016/j.biombioe.2012.12.029.
2. L. Krienitz, E.H. Hegewald, D. Hepperle, V.A.R. Huss, T. Rohr, and M. Wolf, Phylogenetic relationship of Chlorella and Parachlorella gen. nov. (Chlorophyta, Trebouxiophyceae). Phycologia, 2004. 43(5): 529-542.DOI: 10.2216/i0031-8884-43-5-529.1.
3. U. Jena, N. Vaidyanathan, S. Chinnasamy, and K.C. Das, Evaluation of microalgae cultivation using recovered aqueous co-product from thermochemical liquefaction of algal biomass. Bioresource technology, 2011. 102: 3380-7.DOI: 10.1016/j.biortech.2010.09.111.
4. C. Hognon, F. Delrue, J. Texier, M. Grateau, S. Thiery, H. Miller, and A. Roubaud, Comparison of pyrolysis and hydrothermal liquefaction of Chlamydomonas reinhardtii. Growth studies on the recovered hydrothermal aqueous phase. Biomass and Bioenergy, 2015. 73: 23-31.DOI: https://doi.org/10.1016/j.biombioe.2014.11.025.
5. L. Leng, J. Li, Z. Wen, and W. Zhou, Use of microalgae to recycle nutrients in aqueous phase derived from hydrothermal liquefaction process. Bioresource Technology, 2018. 256: 529-542.DOI: https://doi.org/10.1016/j.biortech.2018.01.121.
6. M. Tsarpali, N. Arora, J.N. Kuhn, and G.P. Philippidis, Beneficial use of the aqueous phase generated during hydrothermal carbonization of algae as nutrient source for algae cultivation. Algal Research, 2021. 60: 102485.DOI: https://doi.org/10.1016/j.algal.2021.102485.
7. M.J. Stablein, D.H. Baracho, J.T. Watson, J.C. Silva, Y. Zhang, and A.T. Lombardi, Microalgal photosynthetic inhibition and mixotrophic growth in Post Hydrothermal Liquefaction Wastewater (PHW). Algal Research, 2021. 60: 102548.DOI: https://doi.org/10.1016/j.algal.2021.102548.
8. P. SundarRajan, K.P. Gopinath, J. Arun, K. GracePavithra, A. Adithya Joseph, and S. Manasa, Insights into valuing the aqueous phase derived from hydrothermal liquefaction. Renewable and Sustainable Energy Reviews, 2021. 144: 111019.DOI: https://doi.org/10.1016/j.rser.2021.111019.
9. B. Maddi, E. Panisko, T. Wietsma, T. Lemmon, M. Swita, K. Albrecht, and D. Howe, Quantitative Characterization of Aqueous Byproducts from Hydrothermal Liquefaction of Municipal Wastes, Food Industry Wastes, and Biomass Grown on Waste. ACS Sustainable Chemistry & Engineering, 2017. 5(3): 2205-2214.DOI: 10.1021/acssuschemeng.6b02367.
10. M. Pham, L. Schideman, J. Scott, N. Rajagopalan, and M.J. Plewa, Chemical and Biological Characterization of Wastewater Generated from Hydrothermal Liquefaction of Spirulina. Environmental Science & Technology, 2013. 47(4): 2131-2138.DOI: 10.1021/es304532c.
11. E. Lazzari, K. Arena, E.B. Caramão, P. Dugo, L. Mondello, and M. Herrero, Comprehensive two-dimensional liquid chromatography-based quali-quantitative screening of aqueous

phases from pyrolysis bio-oils. ELECTROPHORESIS, 2021. 42(1-2): 58-67.DOI: https://doi.org/10.1002/elps.202000119.
12. E. Lazzari, K. Arena, E.B. Caramão, and M. Herrero, Quantitative analysis of aqueous phases of bio-oils resulting from pyrolysis of different biomasses by two-dimensional comprehensive liquid chromatography. Journal of Chromatography A, 2019. 1602: 359-367.DOI: https://doi.org/10.1016/j.chroma.2019.06.016.
13. A.S. Kaplitz, M.E. Mostafa, S.A. Calvez, J.L. Edwards, and J.P. Grinias, Two-dimensional separation techniques using supercritical fluid chromatography. Journal of Separation Science, 2021. 44: 426-437.DOI: https://doi.org/10.1002/jssc.202000823.
14. M. Burlet-Parendel and K. Faure, Opportunities and challenges of liquid chromatography coupled to supercritical fluid chromatography. TrAC Trends in Analytical Chemistry, 2021. 144: 116422.DOI: https://doi.org/10.1016/j.trac.2021.116422.
15. M. Sarrut, A. Corgier, G. Cretier, A. Le Masle, S. Dubant, and S. Heinisch, Potential and limitations of on-line comprehensive reversed phase liquid chromatography x supercritical fluid chromatography for the separation of neutral compounds: An approach to separate an aqueous extract of bio-oil. Journal of Chromatography A, 2015. 1402: 124-133.DOI: 10.1016/j.chroma.2015.05.005.
16. D. Guillarme, V. Desfontaine, S. Heinisch, and J.-L. Veuthey, What are the current solutions for interfacing supercritical fluid chromatography and mass spectrometry? Journal of Chromatography B, 2018. 1083: 160-170.DOI: https://doi.org/10.1016/j.jchromb.2018.03.010.
17. C. West, E. Lemasson, S. Bertin, P. Hennig, and E. Lesellier, An improved classification of stationary phases for ultra-high performance supercritical fluid chromatography. Journal of Chromatography A, 2016. 1440: 212-228.DOI: 10.1016/j.chroma.2016.02.052.
18. L.R. Snyder and J.W. Dolan, *High-Performance Gradient Elution: The Practical Application of the Linear-Solvent-Strength Model*, ed. Wiley. 2006, New York, NY.
19. J.M. Davis, D.R. Stoll, and P.W. Carr, Effect of First-Dimension Undersampling on Effective Peak Capacity in Comprehensive Two-Dimensional Separations. Analytical Chemistry, 2008. 80(2): 461-473.DOI: 10.1021/ac071504j.
20. P.G. Stevenson, A. Tarafder, and G. Guiochon, Comprehensive two-dimensional chromatography with coupling of reversed phase high performance liquid chromatography and supercritical fluid chromatography. Journal of Chromatography A, 2012. 1220: 175-178.DOI: https://doi.org/10.1016/j.chroma.2011.11.020.
21. W. Wei, J. Hou, C. Yao, Q. Bi, X. Wang, Z. Li, Q. Jin, M. Lei, Z. Feng, W. Wu, and D. Guo, A high-efficiency strategy integrating offline two-dimensional separation and data post-processing with dereplication: Characterization of bufadienolides in Venenum Bufonis as a case study. Journal of Chromatography A, 2019. 1603: 179-189.DOI: https://doi.org/10.1016/j.chroma.2019.06.037.
22. G. Vivó-Truyols, S. van der Wal, and P.J. Schoenmakers, Comprehensive Study on the Optimization of Online Two-Dimensional Liquid Chromatographic Systems Considering Losses in Theoretical Peak Capacity in First- and Second-Dimensions: A Pareto-Optimality Approach. Analytical Chemistry, 2010. 82(20): 8525-8536.DOI: 10.1021/ac101420f.
23. M. Sarrut, A. D'Attoma, and S. Heinisch, Optimization of conditions in on-line comprehensive two-dimensional reversed phase liquid chromatography. Experimental comparison with one-dimensional reversed phase liquid chromatography for the separation of peptides. Journal of Chromatography A, 2015. 1421: 48-59.DOI: 10.1016/j.chroma.2015.08.052.
24. S.R. Groskreutz and S.G. Weber, Quantitative evaluation of models for solvent-based, on-column focusing in liquid chromatography. Journal of Chromatography A, 2015. 1409: 116-124.DOI: https://doi.org/10.1016/j.chroma.2015.07.038.
25. J. Prothmann, M. Sun, P. Spégel, M. Sandahl, and C. Turner, Ultra-high-performance supercritical fluid chromatography with quadrupole-time-of-flight mass spectrometry (UHPSFC/QTOF-MS) for analysis of lignin-derived monomeric compounds in processed lignin

samples. Analytical and Bioanalytical Chemistry, 2017. 409(30): 7049-7061.DOI: 10.1007/s00216-017-0663-5.
26. K. Vanderlinden, G. Desmet, and K. Broeckhoven, Effect of the feed injection method on band broadening in analytical supercritical fluid chromatography. Journal of Chromatography A, 2020. 1630: 461525.DOI: https://doi.org/10.1016/j.chroma.2020.461525.
27. A.G.-G. Perrenoud, J.-L. Veuthey, and D. Guillarme, Coupling state-of-the-art supercritical fluid chromatography and mass spectrometry: From hyphenation interface optimization to high-sensitivity analysis of pharmaceutical compounds. Journal of Chromatography A, 2014. 1339: 174-184.DOI: 10.1016/j.chroma.2014.03.006.
28. J. Crepier, A. Le Masle, N. Charon, F. Albrieux, P. Duchene, and S. Heinisch, Ultra-high performance supercritical fluid chromatography hyphenated to atmospheric pressure chemical ionization high resolution mass spectrometry for the characterization of fast pyrolysis bio-oils. Journal of Chromatography B, 2018. 1086: 38-46.DOI: https://doi.org/10.1016/j.jchromb.2018.04.005.
29. M. Batteau and K. Faure, Effect of the injection of water-containing diluents on band broadening in analytical supercritical fluid chromatography. Journal of Chromatography A, 2022. 1673: 463056.DOI: https://doi.org/10.1016/j.chroma.2022.463056.
30. M. Camenzuli and P.J. Schoenmakers, A new measure of orthogonality for multi-dimensional chromatography. Analytica Chimica Acta, 2014. 838: 93-101.DOI: http://dx.doi.org/10.1016/j.aca.2014.05.048.
31. W. Nowik, S. Héron, M. Bonose, M. Nowik, and A. Tchapla, Assessment of Two-Dimensional Separative Systems Using Nearest-Neighbor Distances Approach. Part 1: Orthogonality Aspects. Analytical Chemistry, 2013. 85(20): 9449-9458.DOI: 10.1021/ac4012705.
32. N. Nordin, N. Yusof, T. Maeda, N.A. Mustapha, M.Z. Mohd Yusoff, and R.F. Raja Khairuddin, Mechanism of carbon partitioning towards starch and triacylglycerol in Chlorella vulgaris under nitrogen stress through whole-transcriptome analysis. Biomass and Bioenergy, 2020. 138: 105600.DOI: https://doi.org/10.1016/j.biombioe.2020.105600.

615

616 Table 1: Off-line LC x SFC - HRMS conditions

	First dimension (^{1}D)	**Second dimension (^{2}D)**	**HRMS**	
Injection volume	500 µL	10 µL	**Mode**	ESI +/ ESI -
Injection mode	Loop injection	Feed solvent heptane (volume 4 µL; speed 1000 µL/min)	**Mass range (m/z)**	100-1700
Column parameters	Xselect Phenyl hexyl (150 x 4.6 mm, 5 µm)	Torus diol (50 x 3 mm, 1.7 µm)	**Acquisition rate (spectra/s)**	10
Temperature	30 °C	40 °C	**Transient**	761
BPR	N/A	140 bars	**Gas temp (°C)**	300
Flow rate	2.8 mL/min	1.8 mL/min	**Drying gas (l/min)**	11
Mobile phase A	A : H_20	A : CO_2	**Nebulizer (psi)**	40
Mobile phase B	B : ACN	B : EtOH	**Sheat gas temp (°C)**	350
Gradient conditions	1-40 % B in 10 min, 40-1 % B in 0.8 min, 1 % B for 1.2 min	2-50 % B in 1.34 min, 50-2 % B in 0.14 min, 1 % B for 0.46 min	**Sheat Gas Flow (l/min)**	11
Sampling time	0.14 min	N/A	**Capillary voltage (V)**	3500
Make up solvent	N/A	MeOH + 0.1 % FA; 2000 µL/min	**Nozzle voltage (V)**	300
Additional solvent	N/A	MeOH + 0.1 % FA; 200 µL/min	**Fragmentor voltage (V)**	185
Split SFC to MS	N/A	2.7	**Oct 1 RF (Vpp)**	750

617

618

619

620 Table 2. Orthogonality performances using the asterisk equations [27]

Dimension	Asterisk equation	Peak spread
LC dimension	Z1	89%
SFC dimension	Z2	96%
Upward diagonal	Z-	87%
Downward diagonal	Z+	75%
Overall occupation rate	A0	75%

621

622

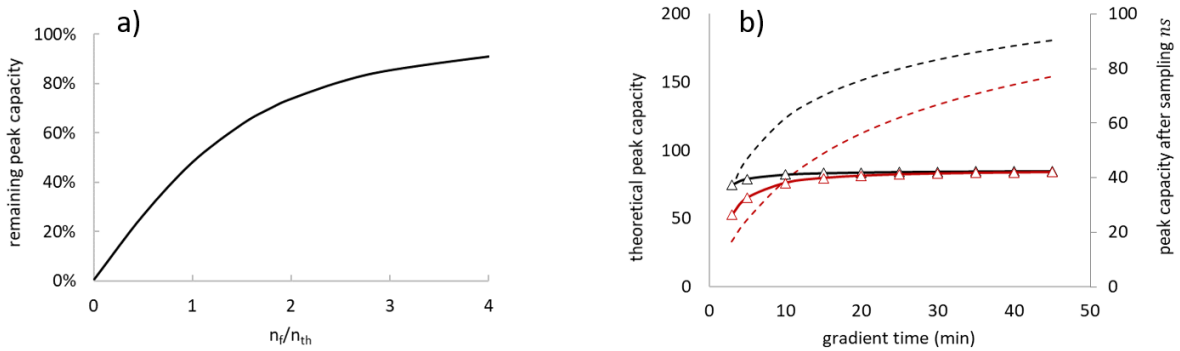

Figure 1. Theoretical performances of the LC dimension. a) plot of the remaining peak capacity vs. the ratio of the number of fractions over theoretical peak capacity $\frac{n_f}{n_{th}}$ (Equation 5); b) plot of the peak capacity as a function of gradient time, for a column with geometry 4.6 x 150 mm, 5 µm, with a gradient running from 1 % to 40 % B, using a flow rate at its optimal value (0.7 mL/min, red marks) or maximal value (2.8 mL/min, black marks), with 80 fractions collected. Left axis is the theoretical peak capacity (dashed lines) and right axis is the effective peak capacity after sampling n_s (plain lines).

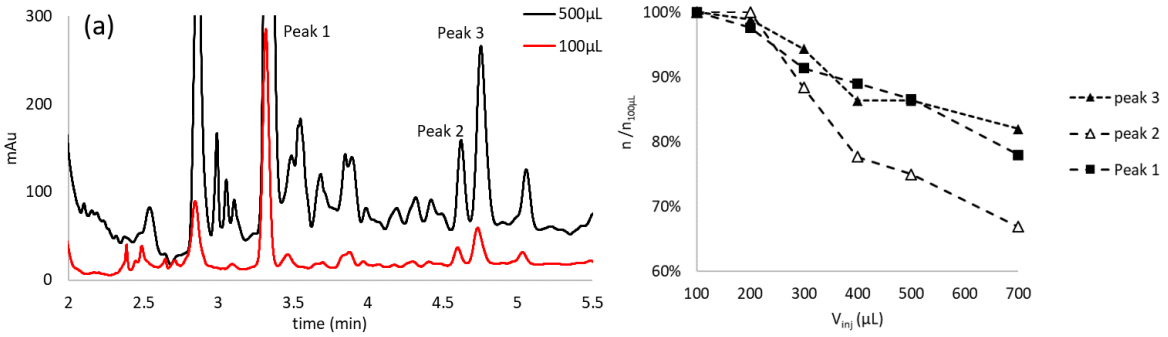

Figure 2. Effect of the injection volume on the RPLC separation of the aqueous phase (a) Overlaid chromatograms with injection volumes of 100 µL (red) and 500 µL (black). (b) Peak capacity loss as a function of injection volume for three different peaks (shown in the top figure). Peak width measured at half peak height. Flow rate: 2.8 mL/min; gradient time: 10 min. UV-detection at 254 nm. Other conditions given in Table 1 (1D conditions).

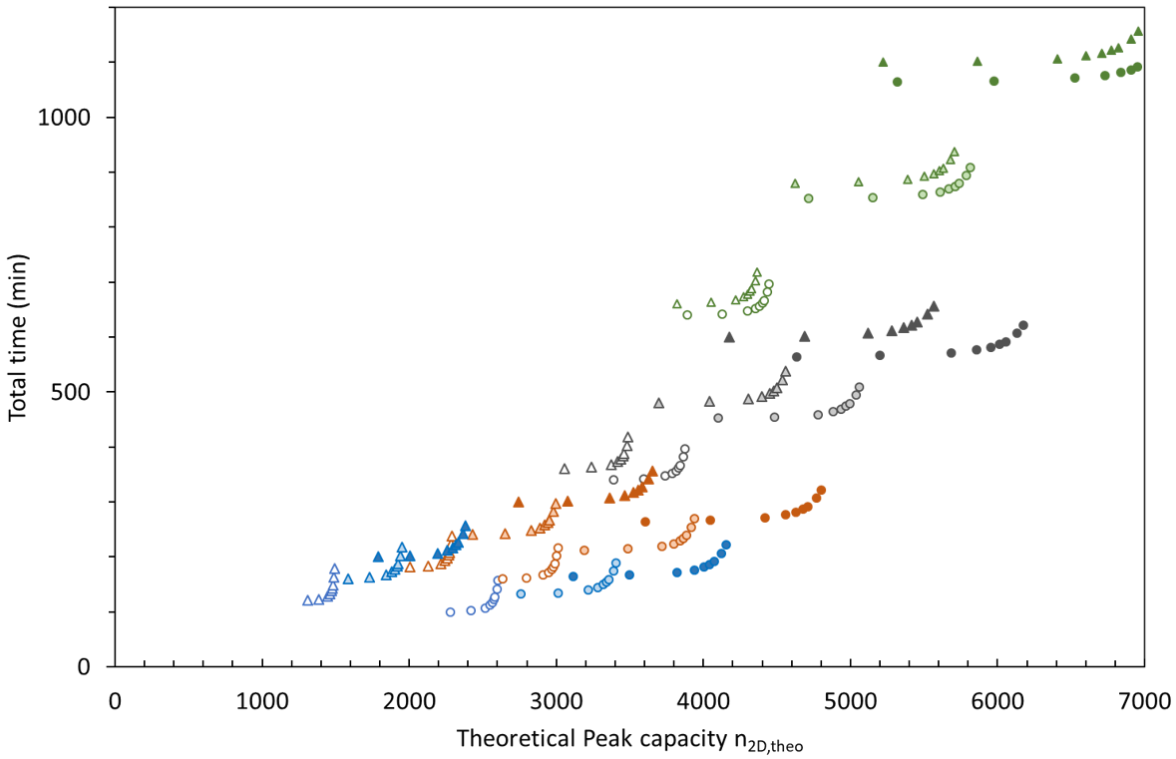

639

640 Figure 3. Theoretical performances of the LC x SFC separation, expressed by a plot of the total time as
641 a function of the 2D theoretical peak capacity. LC flow rate 2.8 mL/min, LC gradient range 3 to 60 min.
642 Fraction number: 60, 80 and 100 (white, light colored and deep colored marks, respectively). SFC
643 gradient time 1 min (blue), 2 min (orange), 5 min (grey) and 10 min (green). SFC column length 50 mm
644 (circle marks) and 100 mm (triangle marks)

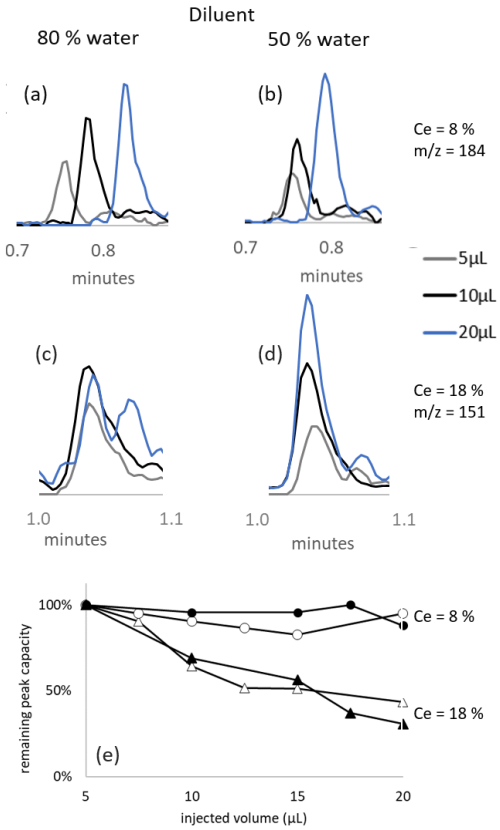

645

646 Figure 4. Effect of the injection in ^{2}D SFC. EIC chromatograms of (a-b) an early eluting peak and (c-d) a
647 late eluting peak when the water/ACN diluent contains (a;c) 80% water or (b;d) 50% water. (e) Loss in
648 peak capacity as a function of injection volume for a diluent 80:20 H_2O/ACN (v/v) (full symbols) and
649 50:50 H_2O/ACN (v/v) (open symbols). Peak width measured at half peak height (FWHM). SFC conditions
650 given in Table 1 (^{2}D conditions). Wastewater was diluted by 10 in the corresponding diluent.

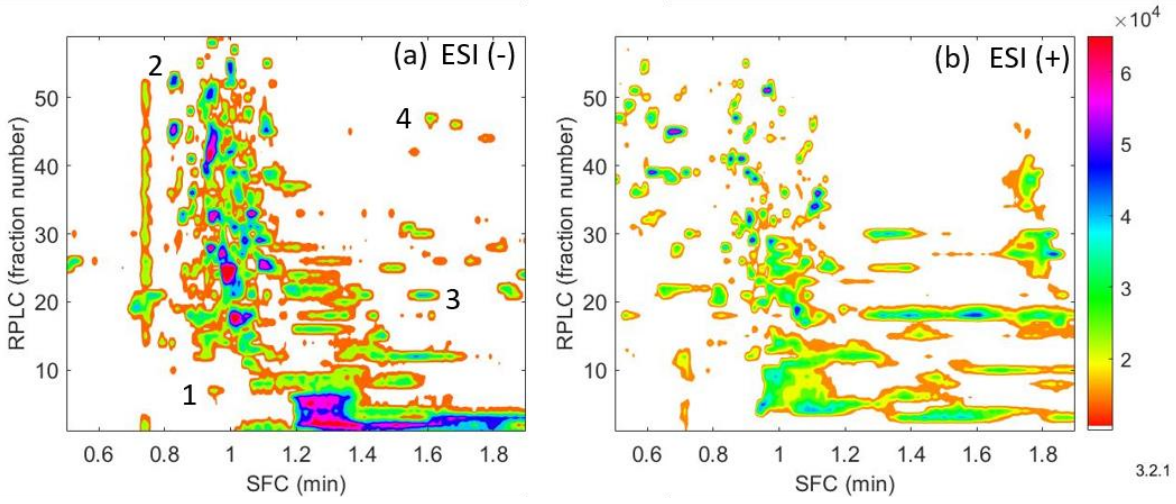

651

652 Figure 5. Base peak chromatograms from the LC x SFC-ESI-HRMS analysis of the wastewater sample,
653 using ESI source in a) negative mode and b) positive mode. Peaks noted 1 to 4 are the monitored
654 isolated peaks spread over the separation space. The experimental conditions are in Table 1.

655

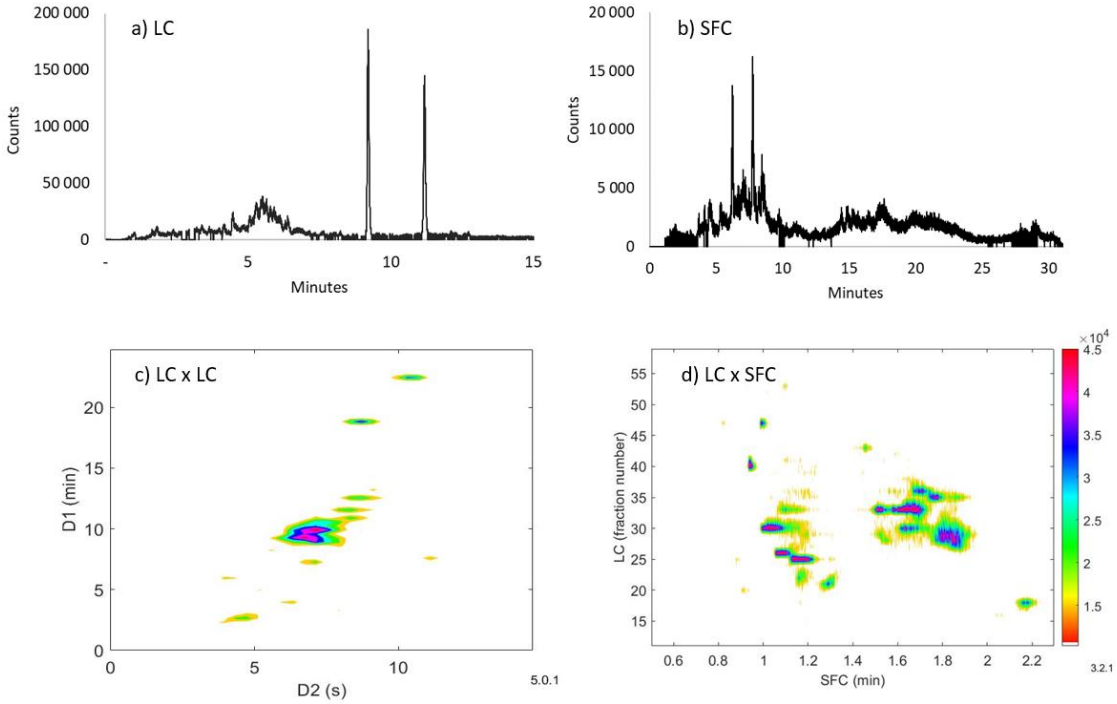

Figure 6. Extracted ion chromatograms at *m/z* 247.1447 for the analysis of *Chlorella sorokiniana* HTL wastewater using a) LC-HRMS, b) SFC-HRMS, c) LCxLC-HRMS and d) LCxSFC -HRMS

Supplementary material

Figure S1. SFC chromatogram of the aqueous phase of algae HTL using various column chemistries. Generic gradient A: CO_2 B: MeOH, 40°C, BPR 140 bar, gradient: 5-50% B, normalized gradient slope 5%, column dimensions 100x3mm, 1.7µm, 1.1 mL/min, V_{inj} 5µL, injection feedsolvent 80/20 Heptane/IPA, UV detection (254nm)

Figure S2. SFC chromatograms of the aqueous phase of algae HTL using a DIOL column and various co-solvents. Gradient A: CO_2 B: co-solvent, 40°C, BPR 140 bar, gradient: 2-50% B, normalized gradient slope 1%, column dimensions 100 x 3 mm, 1.7µm, 1.1 mL/min, V_{inj} 5µL, injection feedsolvent 80/20 Heptane/IPA, UV detection (254 nm)

Figure S3: Theoretical variation of the flow entering the MS, at initial mobile phase composition of 2 % ethanol (blue marks) and final mobile phase composition of 50 % ethanol (grey mark), as a fonction of the flow rate of the make-up pump. Make-up solvent is methanol. Open marks are CO2 flows, plain marks are organic solvent flows. Triangle marks represent the organic solvent flow when no additional pump is used, circle marks are flow values when the additional pump delivers 200 µL/min methanol.

Figure S4 Base peak chromatogram of the aqueous phase of HTL from Sorokiniana Algae, SFC-HRMS obtained with an electrospray source in a) positive mode, b) negative mode, c) UV at 254 nm. Diol column (3 x 50 mm; 1.7 µm), gradient 2% to 50 % EtOH in 1.34 min, 1.8 mL/min, other conditions in Table 1

Figure S5 Base peak chromatogram (ESI+) of the aqueous phase of HTL from Sorokiniana Algae using a) LC phenyl hexyl column, isocratic step at 1 % ACN + 0.1 % formic acid for 1.5 min, then gradient 1%-30% ACN + 0.1 % formic acid in 15 min, 0.5 mL/min, column geometry 2.1 x 100 mm; 1.7 µm, sample diluted by 10 in water, V_{inj} 10 µL. b) SFC Diol column gradient 2% to 50 % EtOH in 30 min, 1.0 mL/min, column geometry 3 x 100 mm; 1.7 µm, BPR 140 bars, 40°C. sample diluted by 3 in ACN/H_2O 50/50. V_{inj} 7 µL. HRMS conditions as in Table 1.

Figure S6. Online LCxLC - Base peak chromatogram of the aqueous phase of HTL from *Chlorella sorokiniana.* First dimension: column geometry 100 x 2.1 mm, 1.7 µm. 30°C, A: water and B: ACN, gradient 1% to 31 % B in 30 min, flow rate 150 µL/min, Vinj 5 µL. Second dimension: column geometry 30 x 2.1 mm, 1.6 µm. 40°C, A: water + 10 mM ammonium acetate and B: MeOH + 10 mM ammonium acetate, gradient 20% to 100% B in 0.21 min, flow rate 2600 µL/min, Vinj 16 µL. Split between first and second dimension by 3. Detection as in Table 1

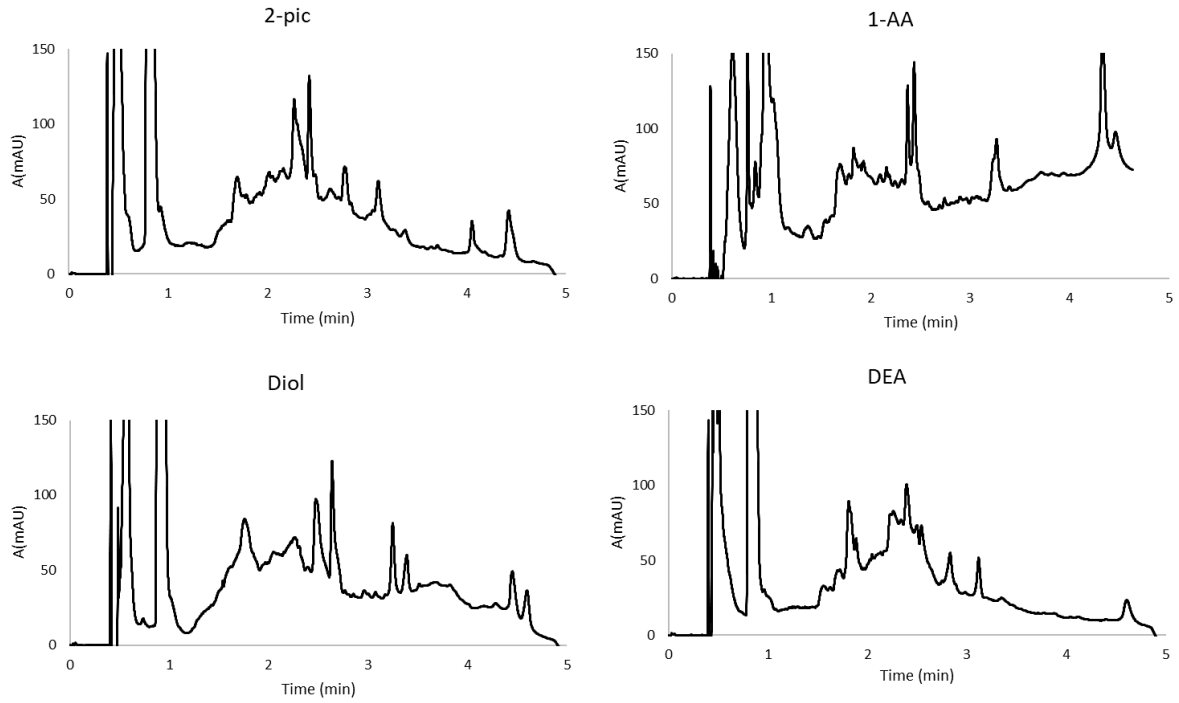

Figure S1. SFC chromatogram of the aqueous phase of algae HTL using various column chemistries. Generic gradient A: CO_2 B: MeOH, 40°C, BPR 140 bar, gradient: 5-50% B, normalized gradient slope 5%, column dimensions 100x3mm, 1.7µm, 1.1 mL/min, V_{inj} 5µL, injection feedsolvent 80/20 Heptane/IPA, UV detection (254nm)

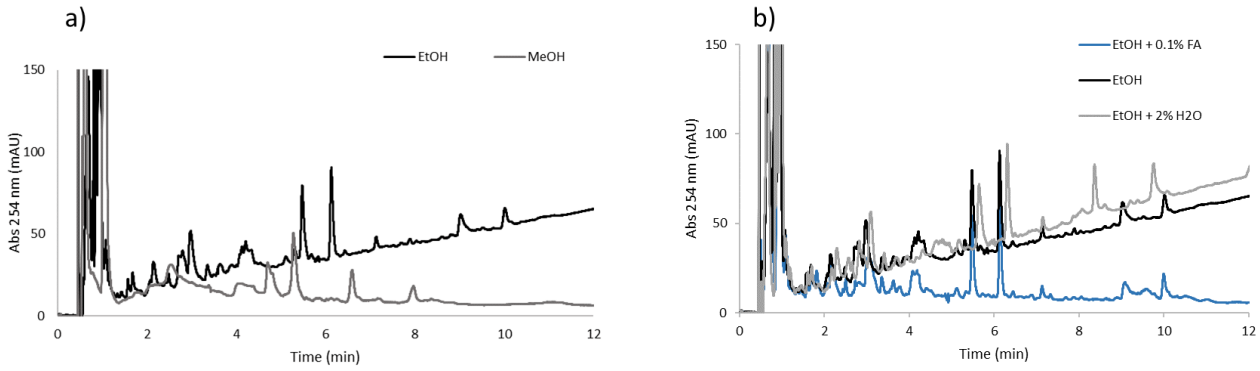

Figure S2. SFC chromatograms of the aqueous phase of algae HTL using a DIOL column and various co-solvents. Gradient A: CO_2 B: co-solvent, 40°C, BPR 140 bar, gradient: 2-50% B, normalized gradient slope 1%, column dimensions 100 x 3 mm, 1.7µm, 1.1 mL/min, V_{inj} 5µL, injection feedsolvent 80/20 Heptane/IPA, UV detection (254 nm)

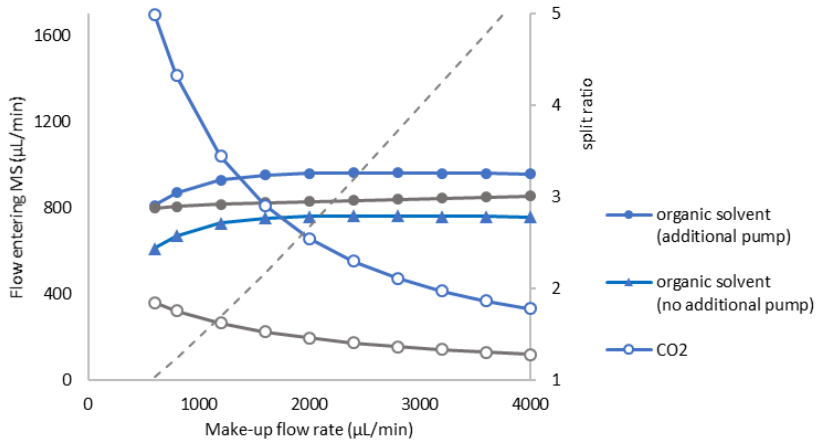

Figure S3: Theoretical variation of the flow entering the MS, at initial mobile phase composition of 2 % ethanol (blue marks) and final mobile phase composition of 50 % ethanol (grey mark), as a fonction of the flow rate of the make-up pump. Make-up solvent is methanol. Open marks are CO2 flows, plain marks are organic solvent flows. Triangle marks represent the organic solvent flow when no additional pump is used, circle marks are flow values when the additional pump delivers 200 µL/min methanol.

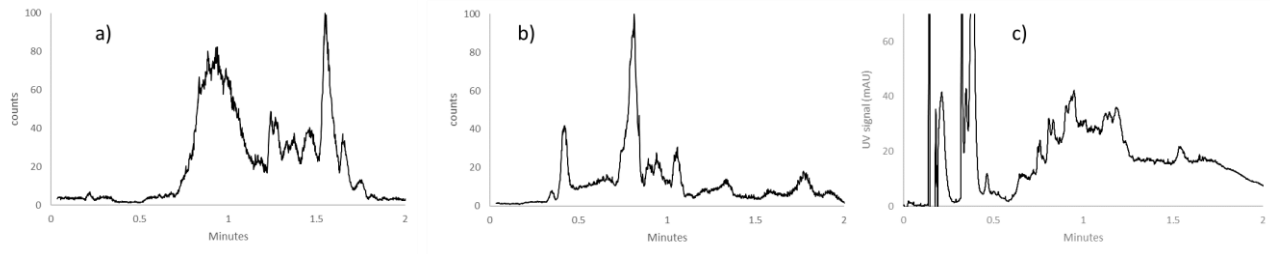

Figure S4 Base peak chromatogram of the aqueous phase of HTL from Sorokiniana Algae, SFC-HRMS obtained with an electrospray source in a) positive mode, b) negative mode, c) UV at 254 nm. Diol column (3 x 50 mm; 1.7 µm), gradient 2% to 50 % EtOH in 1.34 min, 1.8 mL/min, other conditions in Table 1

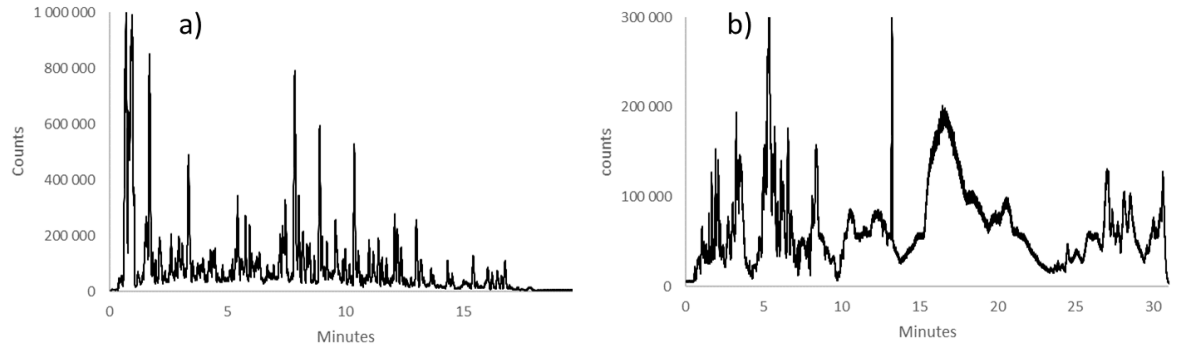

Figure S5 Base peak chromatogram (ESI+) of the aqueous phase of HTL from Sorokiniana Algae using a) LC phenyl hexyl column, isocratic step at 1 % ACN + 0.1 % formic acid for 1.5 min, then gradient 1%-30% ACN + 0.1 % formic acid in 15 min, 0.5 mL/min, column geometry 2.1 x 100 mm; 1.7 µm, sample diluted by 10 in water, V_{inj} 10 µL.

b) SFC Diol column gradient 2% to 50 % EtOH in 30 min, 1.0 mL/min, column geometry 3 x 100 mm; 1.7 µm, BPR 140 bars, 40°C. sample diluted by 3 in ACN/H_2O 50/50. V_{inj} 7 µL. HRMS conditions as in Table 1.

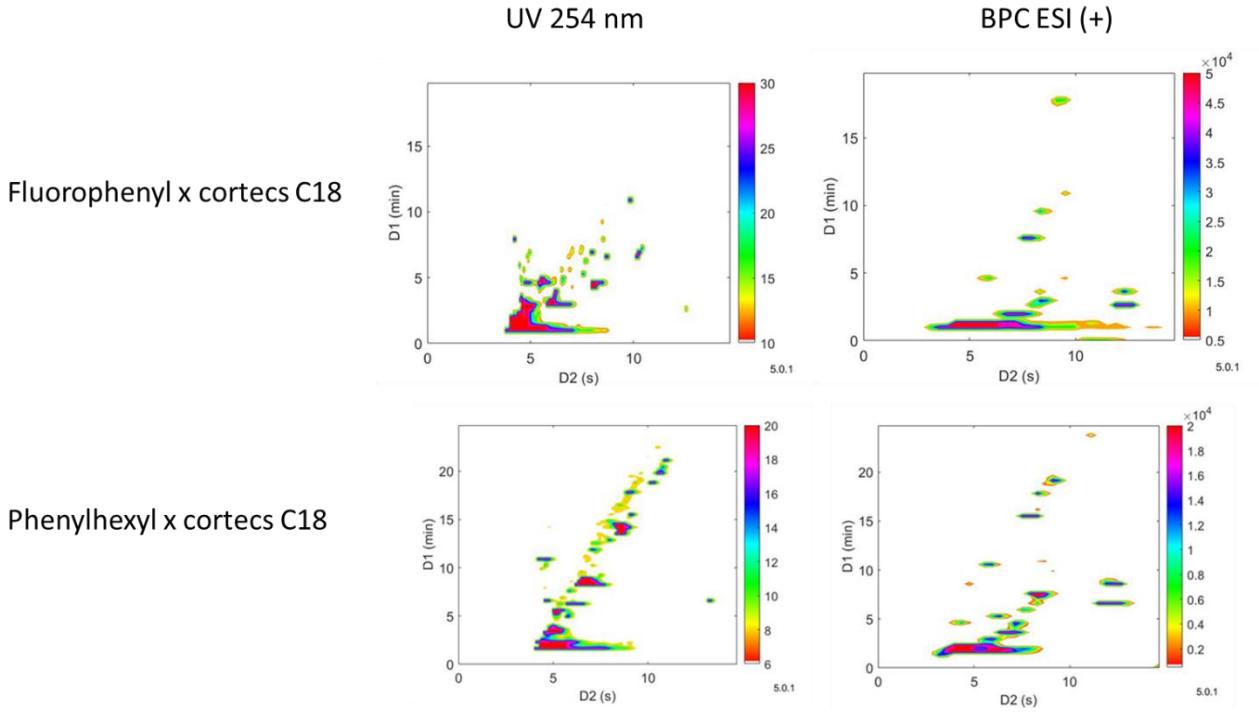

Figure S6. Online LCxLC - Base peak chromatogram of the aqueous phase of HTL from *Chlorella sorokiniana.* First dimension: column geometry 100 x 2.1 mm, 1.7 µm. 30°C, A: water and B: ACN, gradient 1% to 31 % B in 30 min, flow rate 150 µL/min, Vinj 5 µL. Second dimension: column geometry 30 x 2.1 mm, 1.6 µm. 40°C, A: water + 10 mM ammonium acetate and B: MeOH + 10 mM ammonium acetate, gradient 20% to 100% B in 0.21 min, flow rate 2600 µL/min, Vinj 16 µL. Split between first and second dimension by 3. Detection as in Table 1

742

743